

Interface structure and mechanics between graphene and metal substrates: a first-principles study

This article has been downloaded from IOPscience. Please scroll down to see the full text article.

2010 J. Phys.: Condens. Matter 22 485301

(<http://iopscience.iop.org/0953-8984/22/48/485301>)

View [the table of contents for this issue](#), or go to the [journal homepage](#) for more

Download details:

IP Address: 166.111.91.201

The article was downloaded on 25/01/2011 at 09:29

Please note that [terms and conditions apply](#).

Interface structure and mechanics between graphene and metal substrates: a first-principles study

Zhiping Xu¹ and Markus J Buehler^{1,2,3,4}

¹ Laboratory for Atomistic and Molecular Mechanics (LAMM), Department of Civil and Environmental Engineering, Massachusetts Institute of Technology, 77 Massachusetts Avenue, Room 1-235 A&B, Cambridge, MA 02139, USA

² Center for Computational Engineering, Massachusetts Institute of Technology, 77 Massachusetts Avenue, Cambridge, MA 02139, USA

³ Center for Materials Science and Engineering, Massachusetts Institute of Technology, 77 Massachusetts Avenue, Cambridge, MA 02139, USA

E-mail: mbuehler@MIT.EDU

Received 28 July 2010, in final form 13 October 2010

Published 12 November 2010

Online at stacks.iop.org/JPhysCM/22/485301

Abstract

Graphene is a fascinating material not only for technological applications, but also as a test bed for fundamental insights into condensed matter physics due to its unique two-dimensional structure. One of the most intriguing issues is the understanding of the properties of graphene and various substrate materials. In particular, the interfaces between graphene and metal substrates are of critical importance in applications of graphene in integrated electronics, as thermal materials, and in electromechanical devices. Here we investigate the structure and mechanical interactions at a graphene–metal interface through density functional theory (DFT)-based calculations. We focus on copper (111) and nickel (111) surfaces adhered to a monolayer of graphene, and find that their cohesive energy, strength and electronic structure correlate directly with their atomic geometry. Due to the strong coupling between open d-orbitals, the nickel–graphene interface has a much stronger cohesive energy with graphene than copper. We also find that the interface cohesive energy profile features a well-and-shoulder shape that cannot be captured by simple pair-wise models such as the Lennard-Jones potential. Our results provide a detailed understanding of the interfacial properties of graphene–metal systems, and help to predict the performance of graphene-based nanoelectronics and nanocomposites. The availability of structural and energetic data of graphene–metal interfaces could also be useful for the development of empirical force fields for molecular dynamics simulations.

(Some figures in this article are in colour only in the electronic version)

1. Introduction

Recent progress in isolating monolayer graphene sheets and their deposition on various materials as substrates provides not only a powerful scheme to achieve nanoelectronic devices, but can also serve as a test bed to study the structural and transport properties of this two-dimensional material and its interface with other materials [1–3]. Interesting physics have

already been observed in this hybrid system, in particular at graphene–metal interfaces [1, 4, 5]. As an example, the passive graphene layer formed on the nickel surface can protect the underneath spin-polarized electrons against surface adsorptions and chemical oxidation [6, 7]. Understanding of the graphene–substrate interface can further be used to study the interfaces between carbon nanostructures and metallic electrodes in nanoelectronics [8], the mechanism of carbon nanotube or graphene growth [9, 10] and general organic–inorganic interfaces [11].

⁴ Author to whom any correspondence should be addressed.

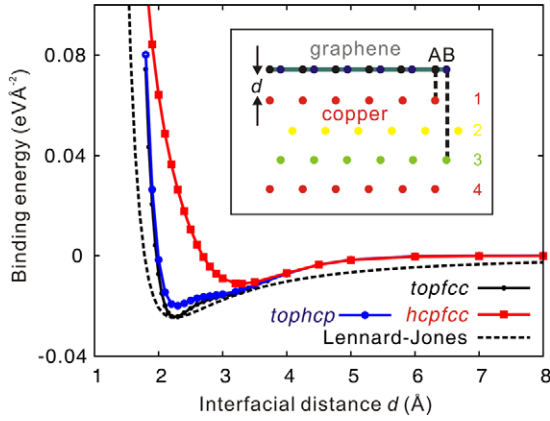


Figure 1. Binding energy of the interface between a graphene monolayer and copper (111) surface as a function of interface distance d . Inset: atomic structure of the interface and metal substrate represented by four atomic layers. There are three configurations with different stacking orders following the terminology in [20], where the two carbon atoms (A and B) in the graphene unit cell cover metal atoms in layers 1 and 3 (topfcc), 1 and 2 (tophcp) or 2 and 3 (hcpfcc). The topfcc configuration has the lowest energy and is thus the most stable one.

On the other hand, low-cost metal–carbon nanotube and metal–graphite nanoplatelet composites are promising solutions for functional materials in digital and high-power electronics applications, which feature reliable mechanical properties and low electrical/thermal resistance [12, 13]. As both carbon nanostructure and copper are good electronic/thermal conductors and widely used in nanoelectronics and nanodevices [14, 15], the rapid advance in this field necessitates a complete picture of their interfacial structural and electronic coupling, which could be the key issue determining their performance for engineering applications [16, 3]. Here we report a series of first-principles studies of graphene–metal interfaces, by considering various metals and their interactions with graphene in order to provide a fundamental perspective of their structure and properties.

2. Materials and methods

The binding between graphene and metal substrates is generally weaker than a covalent bond, and can be classified into two groups. Al, Cu, Ag, Au and Pt have weak cohesion with graphene, while Co, Ni and Pd have strong cohesion [17, 18]. In these substrates, the graphene sheet remains planar rather than corrugated as in sp^3 carbon structures. Our focus is thus placed on the (111) surface of two representative metals, copper and nickel. These two metals are important in both graphene epitaxial growth, nanoelectronics and functional composite applications [10, 6, 7, 19]. Also, copper and nickel (111) surfaces have similar lattice constants as graphene. Thus we choose these two interfaces as test-beds for the graphene–metal substrate interactions.

The interface between graphene and copper is modeled by using a supercell as illustrated in figure 1. The supercell contains one graphene monolayer and a face-centered-cubic (FCC) metal substrate in the (111) direction. A vacuum layer of 20 Å is used in the direction normal

Table 1. Structure (interface distance d_{C-M}) and properties (interface binding energy E_b and mechanical strength σ_s) of the interface between graphene and metal substrates.

Metal	d_{C-M} (Å)	E_b (meV Å ⁻²)	σ_s (GPa)
C–Cu	2.243	24.81	2.92
C–Cu (a_g) ^a	3.260	13.19	—
C–Ni	2.018	91.33	18.70

^a Lattice constant of graphene instead of metal substrates is used.

to the interface, representing the isolated slab boundary condition. The structures and properties of this hybrid system are subsequently investigated using plane-wave basis-set-based density functional theory (DFT) methods. The local (spin) density approximation (LDA) and generalized gradient approximation (GGA) are well known to overbind and underbind, thus giving different values for binding distance and energy. Although GGA offers better predictions for both graphene and metals, it gives incorrect binding behavior for the graphene–metal interfaces [20, 21]. Thus in our work the LDA is applied instead of GGA.

We use the Quantum ESPRESSO package (<http://quantum-espresso.org/>) for all calculations reported here, equipped with Perdew–Zunger pseudopotential parameters [22]. For all results presented, energy cutoffs of 30 and 240 Ryd are used for plane-wave basis sets and charge density grids, respectively. 32 Monkhorst–Pack sampling k -points are used in each in-plane direction for Brillouin zone integration. These settings have been verified to achieve a total energy convergence less than 1 meV/atom. For geometry relaxation, the force on atoms is converged below a threshold of 0.01 eV Å⁻¹.

3. Results and discussion

Figure 1 shows the optimized atomic structure of the graphene–copper (111) interface. Corresponding geometric parameters and physical properties are summarized in table 1. In the experiments, a metal substrate is usually much thicker than the graphene, thus the hybrid system features a lattice constant close to that of the metal. Because of the well-known deficiency of LDA that results in an underestimation of the lattice constants, we used the experimentally measured FCC lattice constants of the metals (3.61 Å for copper and 3.52 Å for nickel) to determine the in-plane periodicity of the hybrid system. In this situation, a pre-strain in graphene is introduced that is 4.6% for graphene–copper and 2% at the graphene–nickel interface. According to the experimental evidence, this mismatch will not induce out-of-plane buckling and the flat interface will be retained for copper and nickel, in contrast to other metals such as ruthenium where ripples form to release the pre-stress [19, 10, 1]. Thus we expect that the supercell approach utilized here gives a reasonable description of the interface structure.

Our calculation results firstly show that the cohesion between graphene and the copper (111) surface depends remarkably on their stacking geometry. According to the relative positions of graphene sublattices A and B (figure 1)

with respect to the metal surface, we define the interface configuration as tophcp when A(B) overlaps with the first (second) layer in the substrate, topfcc when A(B) overlap with the first (third) layer in the substrate and hcpfcc when A(B) overlap with the second (third) layer in the substrate [20]. To quantitatively characterize the interface mechanical properties, the binding energy between the graphene sheet and metal substrate is calculated as $E_b = E_{C-M} - (E_C + E_M)$, where E_{C-M} , E_C and E_M are energies of the hybrid system, isolated graphene monolayer and metal substrate, respectively.

The results depicted in figure 1 show that the topfcc configuration is the most stable one, with a cohesive energy of $E_b = -24.81 \text{ meV } \text{\AA}^{-2}$, while the tophcp and hcpfcc cases have cohesive energies of $E_b = -20.20$ and $-11.16 \text{ meV } \text{\AA}^{-2}$. We also calculate the potential energy surface between graphene and metal, by separating the graphene sheet rigidly from the uppermost metal atom layer without further internal geometry relaxation in graphene and metal layers. We find that, except for the hcpfcc, both tophcp and topfcc configurations have a well-and-shoulder potential profile (figure 1), which is unexpected based on conventional and widely used pair-wise interatomic interaction models. This profile can be superposed by two single-well potential profiles with minima at 2.24 and 3.26 \AA . The small slope of the energy profile between these two distances suggests a rather soft interfacial cohesion.

In previous atomistic simulations of graphene-metal interfaces, empirical potential functions such as the Lennard-Jones form $A_0/d^{12}-B_0/d^6$ were used to describe van der Waals type interactions, where A_0 and B_0 are material-specific coefficients [23, 24]. This expression gives an interlayer binding energy function as $E_b(d) = a/d^8 - b/d^2$. Using the binding energy $E_b = -24.81 \text{ eV } \text{\AA}^{-2}$ at the equilibrium distance $d = 2.24$, we can fit the binding energy for the topfcc configuration as $a = 29.8604 \text{ eV } \text{\AA}^8$, $b = 0.9368 \text{ eV } \text{\AA}^2$. However, as clearly shown in figure 1, this Lennard-Jones form cannot capture the well-and-shoulder feature of the potential profile. Firstly, the Lennard-Jones formula is concave at one minimum, while the DFT-derived energy profile is a superposition of two single-well curves with separated minima. Secondly, the tail of the fitting function decays much too slowly in comparison to the DFT-based calculation results, which fit well into exponential functions, revealing a deficiency of state-of-the-art DFT methods.

Based on the data shown in figure 1 we find that the well-and-shoulder feature does not show up in the hcpfcc configuration, where the carbon atoms do not overlap with metal atoms in the first layer. Thus the interaction between graphene and the first metal layers could be the origin of the potential well at 2.24 \AA . To investigate this issue further we also calculate the Lennard-Jones binding energy between a graphene sheet and four metal layers based on an atom-by-atom summation approach. For the hcpfcc, topfcc and tophcp configurations, the result does not show the well-and-shoulder feature, but displays single-well profiles. We conclude that, in the Lennard-Jones formula, the interaction between graphene and the first metal layer is not strong enough relatively to create a dip in the potential profile, in comparison with the second, third and fourth layers at larger distances. In other words,

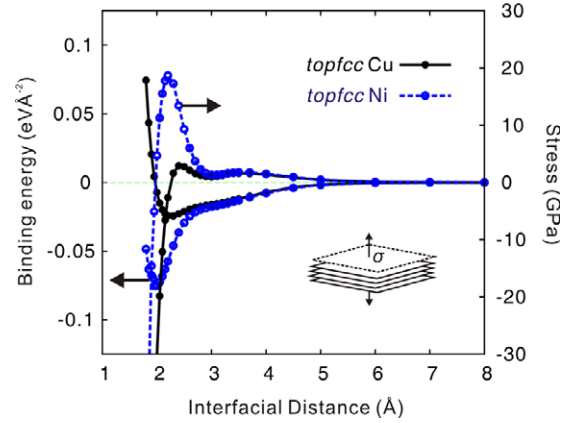


Figure 2. Interface binding energy and stress σ between graphene and the copper/nickel (111) surfaces. The binding energy E_b is $-91.33 \text{ meV } \text{\AA}^{-2}$ for nickel, higher than $-24.81 \text{ eV } \text{\AA}^{-2}$ for the copper surface. Its tensile strength is 18.70 GPa, also much higher than 2.92 GPa as obtained for the copper surface.

the interacting mechanism between graphene and first layer metal atoms could have a unique nature, that is, from a charge-transfer-induced short-range electrostatic interaction.

To facilitate a direct comparison with copper, we investigate the strongly bonded interface between graphene and a nickel (111) surface. The potential energy profile shows a similar characteristic as in the previous case. However, the binding energy here is much deeper, i.e. $E_b = -91.33 \text{ meV } \text{\AA}^{-2}$, although their interface distance at equilibrium is similar. We also calculate the energy profile by separating one isolated carbon atom from metal surfaces, where the double-minima characteristic is absent. Thus it must arise from the π and π^* orbitals in graphene and their coupling with the metal states.

In the optimized topfcc structure, the distance between graphene and metal is 2.24 \AA for copper and 2.018 \AA for nickel. This distance is close to the values of the interlayer distance in metals, which is 2.08 \AA in copper and 2.03 \AA in nickel, implying an electrostatic nature of the interlayer interaction. We also perform calculations using graphene's lattice constant $a_g = 2.44 \text{ \AA}$ for the hybrid system, which represents the case where metal atoms are deposited on graphene. However, an interface distance of 3.26 \AA is obtained with cohesive energy $E_b = -13.19 \text{ meV } \text{\AA}^{-2}$, in agreement with previous reports [18, 17]. This strain-dependent binding property suggests that mechanical deformation can be applied to tune the interface properties.

The range of coupling states at the interface is now studied by using a bilayer graphene sheet on top of the copper substrate. After geometry optimization, the distance between the bottom graphene layer and copper (111) surface is still 2.24 \AA : however, the interlayer distance between two graphene sheets is 3.26 \AA , close to the interlayer distance in graphite. This result shows that the interface coupling is spatially localized below the bottom graphene layer.

The mechanical properties at the interfaces are quantified through stress-strain curves as shown in figure 2. We define the interface stress as $\sigma = F_{C-M}/A$, where F_{C-M} is the

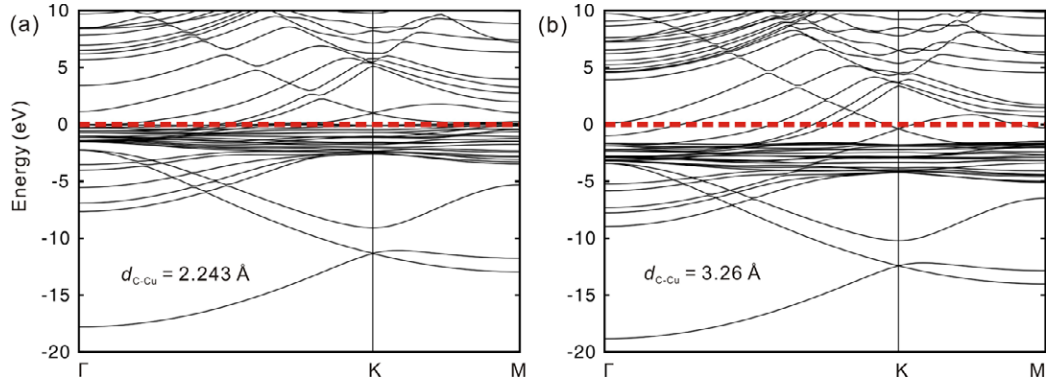


Figure 3. Electronic band structure of the graphene–copper (111) hybrid system with interface distance $d_{C-Cu} = 2.243 \text{ \AA}$ (a) and 3.26 \AA (b). The results show that at $d_{C-Cu} = 2.243 \text{ \AA}$ the Fermi level is pinned to the Cu bands, while at $d_{C-Cu} = 3.26$, the coupling between the p_z orbital of carbon atoms and the d_{z^2} orbital of copper atoms is weak, and the Fermi level is close to the crossing between graphene π and π^* bands.

force acting on a graphene layer that is also equal to the force applied to the metal substrate. The graphene–Ni (111) interface has a much higher tensile strength $\sigma_s = 18.70 \text{ GPa}$ than 2.92 GPa for the graphene–Cu(111) interface. For both interfaces, the convex portion of the energy profile between two energy minima lowers the stress considerably. To explain this, we project the force exerted on the graphene layer into sublattices A and B, and calculate the corresponding stress σ_A and σ_B . The result shows that the stress on sublattice A overlaps the first layer of metal, its strength σ_A maximizes at $d = 2.24 \text{ \AA}$, while σ_B has two local maximal values and the higher one is located at $d = 3.26 \text{ \AA}$. The symmetry between sublattices A and B is thus broken due to the coupling with metal states and results in the novel binding properties shown above.

In order to obtain more insights into the difference in binding strength between copper and nickel, and their relationship to the electronic structures, we further analyze the electronic coupling across the interface. We plot the band structures of graphene–Cu(111) system with different interlayer distances $d = 2.243$ and 3.26 \AA (figure 3). The results show that at $d_{C-Cu} = 2.243 \text{ \AA}$ the Fermi level is pinned to the Cu bands, i.e. electrons are transferred from π bands in the graphene layer into metal bands, while at $d_{C-Cu} = 3.26$, the coupling between the p_z orbital of carbon atoms and the d_{z^2} orbital of copper atoms is weak, and electrons in metal bands are now transferred into the graphene layer. Consequently, the Fermi level is now close to the crossing between graphene π and π^* bands. After projecting the band structure to the p_z orbital on carbon atoms and the d_{z^2} orbital on copper atoms, we find that, except for the observed charge transfer between graphene and metal orbitals, their coupling is very weak so that the characterized feature of the π and π^* bands is not perturbed. Instead, in the graphene–Ni (111) system, a strong coupling is observed and the band structure of graphene is severely perturbed. This interaction between p_z electrons in graphene and open d-orbitals in nickel (which is absent in copper) is responsible for the difference in interface binding properties. Additional calculations (results not presented here) show that iron and cobalt also have strong binding with

graphene sheets due to their open d-orbitals. This suggests that, in designing metal–carbon-based composites, the thermal and electrical transfer properties can be tuned by using different metal matrices [3, 13].

4. Conclusion

In conclusion, we find that the interface mechanical properties between graphene and metal substrates is markedly different from predictions from simple pair-wise potential functions such as the Lennard-Jones formula. This behavior, which is absent even in the case when a carbon atom binds to a metal surface, arises from the details of the electronic coupling between graphene and metal, especially the first layer that has direct charge transfer with the graphene layer. The broken symmetry between sublattices A and B in graphene and their relative positions to the metal atoms below leads to an effective potential profile that can be understood based on the superposition of two adhesion–repulsion curves with different minima corresponding to interlayer distances in graphite and bulk metal. We find that the cohesive energy and strength between graphene and Ni(111) surfaces is much higher than for Cu(111) surfaces due to the coupling between the p_z orbital in the graphene layer and the d_{z^2} orbital in metal for Ni(111), while on Cu(111) surfaces only the charge transfer process is observed. The strong dependence of the binding properties with respect to metal elements, interface structure and in-plane strain, as observed here, has important implications in functional nanocomposites with tunable mechanical, thermal and electrical properties.

There are some general concerns regarding the validity of density functional theory with the local density approximation or generalized gradient approximation for a hybrid system as considered here. The recently developed van der Waals functional that includes nonlocal correlations was applied to this interface and it is noted that some results obtained with this model are in conflict with experimental measurements [21]. For example, it results in an incorrect binding distance $d = 3.50 \text{ \AA}$ between graphene and nickel, while the experimental measurement is 2.1 \AA [21]. On the other hand, LDA

gives a reasonably accurate description of the graphene–nickel interface and the interlayer coupling in graphite [21, 25]. This may arise from the nature of the π -orbital coupling at the interface instead of polarization on neutral atoms [26]. As it is difficult to develop a precise functional for both bulk materials (metals, semiconductors and insulators) and their interfaces, high-level quantum chemistry calculations or direct experimental measurement could be used to characterize the interface properties in future studies.

In conclusion, the results reported here suggest that special attention must be paid when using an empirical force field to capture the complicated potential surface at the interface, which is currently widely applied to several fields including nanoelectronics and carbon nanostructure growth [27]. As an alternative approach to the method used here, the tight-binding model (with an empirical quantum mechanical description of electronic structure) could be utilized for large-scale molecular dynamics simulations after fitting corresponding parameters from the DFT results [28, 29].

Acknowledgments

This work was supported by DARPA and the MIT Energy Initiative (MITEI).

References

- [1] Wintterlin J and Bocquet M L 2009 Graphene on metal surfaces *Surf. Sci.* **603** 1841–52
- [2] Zhou S Y, Gweon G H, Fedorov A V, First P N, de Heer W A, Lee D H, Guinea F, Castro Neto A H and Lanzara A 2007 Substrate-induced bandgap opening in epitaxial graphene *Nat. Mater.* **6** 770–5
- [3] Xu Z and Buehler M J 2009 Nanoengineering heat transfer performance at carbon nanotube interfaces *ACS Nano* **3** 2767–75
- [4] Sutter P W, Flege J-I and Sutter E A 2008 Epitaxial graphene on ruthenium *Nat. Mater.* **7** 406–11
- [5] Gao M, Pan Y, Zhang C D, Hu H, Yang R, Lu H L, Cai J M, Du S X, Liu F and Gao H J 2010 Tunable interfacial properties of epitaxial graphene on metal substrates *Appl. Phys. Lett.* **96** 053109
- [6] Yu S D, Fonin M and Laubschat C 2008 A possible source of spin-polarized electrons: the inert graphene/Ni(111) system *Appl. Phys. Lett.* **92** 052506
- [7] Yu S D, Fonin M, Rudiger U and Laubschat C 2008 Graphene-protected iron layer on Ni(111) *Appl. Phys. Lett.* **93** 022509
- [8] Barraza-Lopez S, Vanevic M, Kindermann M and Chou M Y 2010 Effects of metallic contacts on electron transport through graphene *Phys. Rev. Lett.* **104** 076807
- [9] Ding F, Larsson P, Larsson J A, Ahuja R, Duan H, Rosen A and Bolton K 2007 The importance of strong carbon–metal adhesion for catalytic nucleation of single-walled carbon nanotubes *Nano Lett.* **8** 463–8
- [10] Li X, Cai W, Colombo L and Ruoff R S 2009 Evolution of graphene growth on Ni and Cu by carbon isotope labeling *Nano Lett.* **9** 4268–72
- [11] Czaja A U, Trukhan N and Mueller U 2009 Industrial applications of metal–organic frameworks *Chem. Soc. Rev.* **38** 1284–93
- [12] Xu C, Wang X and Zhu J 2008 Graphene–metal particle nanocomposites *J. Phys. Chem. C* **112** 19841–5
- [13] Stankovich S, Dikin D A, Dommett G H B, Kohlhaas K M, Zimney E J, Stach E A, Piner R D, Nguyen S T and Ruoff R S 2006 Graphene-based composite materials *Nature* **442** 282–6
- [14] Xu Z and Buehler M J 2009 Strain controlled thermomutability of single-walled carbon nanotubes *Nanotechnology* **20** 185701
- [15] Xu Z, Zheng Q-S and Chen G 2007 Elementary building blocks of graphene-nanoribbon-based electronic devices *Appl. Phys. Lett.* **90** 223115
- [16] Xu Z and Buehler M J 2009 Hierarchical nanostructures are crucial to mitigate ultrasmall thermal point loads *Nano Lett.* **9** 2065–72
- [17] Karpan V M, Giovannetti G, Khomyakov P A, Talanana M, Starikov A A, Zwierzycki M, van den Brink J, Brocks G and Kelly P J 2007 Graphite and graphene as perfect spin filters *Phys. Rev. Lett.* **99** 176602
- [18] Giovannetti G, Khomyakov P A, Brocks G, Karpan V M, van den Brink J and Kelly P J 2008 Doping graphene with metal contacts *Phys. Rev. Lett.* **101** 026803
- [19] Li X *et al* 2009 Large-area synthesis of high-quality and uniform graphene films on copper foils *Science* **324** 1312–4
- [20] Miguel F-C, Baskes M I, Anatoli V M and Michael L S 2008 Bridge structure for the graphene/Ni(111) system: a first principles study *Phys. Rev. B* **77** 035405
- [21] Vanin M, Mortensen J J, Kelkkanen A K, Garcia-Lastra J M, Thygesen K S and Jacobsen K W 2010 Graphene on metals: a van der Waals density functional study *Phys. Rev. B* **81** 081408
- [22] Giannozzi P *et al* 2009 Quantum Espresso: a modular and open-source software project for quantum simulations of materials *J. Phys.: Condens. Matter* **21** 395502
- [23] Wang L, Zhang H W, Zheng Y G, Wang J B and Zhang Z Q 2008 Single-walled carbon nanotubes filled with bimetallic alloys: structures and buckling behaviors *J. Appl. Phys.* **103** 083519
- [24] Guo Y F and Guo W L 2006 Structural transformation of partially confined copper nanowires inside defected carbon nanotubes *Nanotechnology* **17** 4726–30
- [25] Hasegawa M and Nishidate K 2004 Semiempirical approach to the energetics of interlayer binding in graphite *Phys. Rev. B* **70** 205431
- [26] Zaremba E and Kohn W 1976 van der Waals interaction between an atom and a solid surface *Phys. Rev. B* **13** 2270–85
- [27] Liu B, Lusk M T, Ely J F, van Duin A C T and Goddard W A 2008 Reactive molecular dynamics force field for the dissociation of light hydrocarbons on Ni(111) *Mol. Simul.* **34** 967–72
- [28] Sutton A P 1988 The tight-binding bond model *J. Phys. C: Solid State Phys.* **21** 35
- [29] Carlson A and Dumitrică T 2007 Extended tight-binding potential for modelling intertube interactions in carbon nanotubes *Nanotechnology* **18** 065706